HHS Public Access

Author manuscript

Leukemia. Author manuscript; available in PMC 2015 October 01.

Published in final edited form as:

Leukemia. 2015 April ; 29(4): 807–818. doi:10.1038/leu.2014.296.

A regimen combining the Wee1 inhibitor AZD1775 with HDAC inhibitors targets human acute myeloid leukemia cells harboring various genetic mutations

Liang Zhou[1,*], **Yu Zhang**[1,2,*], **Shuang Chen**[1], **Maciej Kmieciak**[1], **Yun Leng**[1,3], **Hui Lin**[1], **Kathryn A. Rizzo**[4], **Catherine I. Dumur**[4], **Andrea Ferreira-Gonzalez**[4], **Yun Dai**[1,†], and **Steven Grant**[1,5,†]

[1]Division of Hematology and Oncology, Department of Medicine, Virginia Commonwealth University and the Massey Cancer Center, Richmond, VA 23298, USA

[2]National Engineering Laboratory for Druggable Gene and Protein Screening, Northeast Normal University, Changchun, Jilin 130024, China

[3]Department of Hematology, Beijing Chaoyang Hospital of Capital Medical University, Beijing 100020, China

[4]Division of Molecular Diagnostics, Department of Pathology, Virginia Commonwealth University and the Massey Cancer Center, Richmond, VA 23298, USA

[5]Department of Biochemistry, Virginia Commonwealth University and the Massey Cancer Center and Institute of Molecular Medicine, Richmond, VA 23298, USA

Abstract

AZD1775 targets the cell cycle checkpoint kinase Wee1 and potentiates genotoxic agent cytotoxicity through p53-dependent or -independent mechanisms. Here, we report that AZD1775 interacted synergistically with histone deacetylase inhibitors (HDACIs e.g., Vorinostat), which interrupt the DNA damage response (DDR), to kill p53-wild type or -deficient as well as FLT3-ITD leukemia cells in association with pronounced Wee1 inhibition and diminished cdc2/Cdk1 Y15 phosphorylation. Similarly, Wee1 shRNA knock-down significantly sensitized cells to HDACIs. While AZD1775 induced Chk1 activation, reflected by markedly increased Chk1 S296/

†Corresponding authors: Dr. Steven Grant, Division of Hematology/Oncology, P.O. Box 980035, Virginia Commonwealth University, Richmond, VA 23298, Phone: 804-828-5211, Fax: 804-828-8079, stgrant@vcu.edu. Dr. Yun Dai, Virginia Commonwealth University and the Massey Cancer Center, Room 234 Goodwin Research Building, 401 College Street, Richmond VA 23298, Phone: 804-828-5168, Fax: 804-827-3781, ydai@vcu.edu.

*These authors contributed equally to this work.

CONFLICT OF INTEREST

No potential conflicts of interest were disclosed.

AUTHOR CONTRIBUTION

YD, SG conceptualized research and formed the hypothesis of this paper; SC, YD designed, performed experiments, analyzed data; LZ, YZ, SC, YL, HL, YD performed the *in vitro* research and collected data; LZ, YZ, SC, YD performed animal studies and collected data; MK designed, performed and analyzed flow cytometry work; KAR, CID, AF-G provided patient samples, or performed and analyzed NGS work; YD, SG wrote the manuscript.

Supplementary information is available at Leukemia's website.

S317/S345 phosphorylation leading to inhibitory T14 phosphorylation of cdc2/Cdk1, these compensatory responses were sharply abrogated by HDACIs. This was accompanied by premature mitotic entry, multiple mitotic abnormalities, and accumulation of early S-phase cells displaying increased newly replicated DNA, culminating in robust DNA damage and apoptosis. The regimen was active against patient-derived AML cells harboring either wild type or mutant p53, and various NGS-defined mutations. Primitive $CD34^+/CD123^+/CD38^-$ populations enriched for leukemia-initiating progenitors, but not normal $CD34^+$ hematopoietic cells, were highly susceptible to this regimen. Finally, combining AZD1775 with Vorinostat in AML murine xenografts significantly reduced tumor burden and prolonged animal survival. A strategy combining Wee1 with HDACI inhibition warrants further investigation in AML with poor prognostic genetic aberrations.

Keywords

Wee1 inhibitor; HDAC inhibitor; Chk1; cdc2/Cdk1; checkpoint; AML

INTRODUCTION

Acute myelogenous leukemia (AML) is a stem cell disorder resulting from differentiation and cell death program defects. Despite progress in elucidating AML molecular pathogenesis (1) and introduction of novel agents targeting mutant oncoproteins implicated in leukemogenesis (e.g., FLT3-ITD) (2), the prognosis of patients with relapsed/refractory disease, particularly those ineligible for bone marrow transplantation, remains grim (3). This has stimulated the development of epigenetically-based therapies in AML, including DNMT1 and histone deacetylase inhibitors (HDACIs) (4). HDACIs induce histone tail acetylation and an open chromatin structure favoring expression of cell differentiation or death genes (5). HDACIs have shown significant pre-clinical activity in AML, and some, albeit limited, single agent activity (4). Notably, the FDA has recently granted Orphan Drug designation to the HDACI Pracinostat in AML (6). Moreover, combining HDACIs e.g., Vorinostat, approved for CTCL, with standard cytotoxic regimens exhibits pronounced activity in AML (7).

HDACI lethality toward AML and other tumor types stems from multiple actions, including death receptor up-regulation, reactive oxygen species generation, and up-regulation of pro-apoptotic proteins (e.g., Bim), among others (8). Recently, attention has focused on HDACI-mediated disruption of the DNA damage response (DDR) (9, 10). HDACIs down-regulate Chk1 (11, 12), a kinase critical for all cell cycle checkpoints (13), as well as DNA repair (14) in neoplastic cells. Notably, AML cells expressing mutant/fusion oncoproteins (e.g., FLT3-ITD, leukemia-associated fusion protein/LAFPs) which exhibit intrinsic DDR defects (15), may be particularly vulnerable to HDACIs (16).

Evidence that HDACIs selectively induce DNA damage in neoplastic cells (9), including leukemia cells (17), impair the DDR (e.g., checkpoints and repair) (8), and identification of Wee1, a protein kinase principally involved in regulation of the G2/M checkpoint by phosphorylating cyclin-dependent kinase 1 (cdc2/Cdk1) at the inhibitory residue Y15 (18),

as a novel therapeutic target in AML (19, 20), provide a rationale for combined Wee1/HDAC inhibition in AML. Here we report that AZD1775, a highly selective small molecule ATP-competitive Wee1 inhibitor currently undergoing clinical evaluation (21), interacts synergistically with HDACIs *in vitro and in vivo* in AML cells in association with Wee1 inhibition, Chk1-mediated checkpoint abrogation, premature mitotic entry, and increased DNA damage. Notably, cells expressing either wild-type or mutant p53, including those carrying FLT3 mutations (e.g., FLT3-ITD), are highly susceptible to this strategy, as are primary AML cells but not normal hematopoietic cells. Collectively, these findings argue that a strategy combining Wee1 with HDAC inhibitors warrants further evaluation in AML.

MATERIALS AND METHODS

Cells and reagents

Human AML cell lines U937 (p53-null), MV4-11 (p53-mutated, FLT3-ITD), MOLM-13 (p53 wild-type, FLT3-ITD), and OCI-AML3 (p53 wild-type) were maintained as before (12). Experiments utilized logarithmically growing cells (3–6 × 10^5 cells/ml). Bone marrow (BM) or peripheral blood (PB) samples were obtained with informed consent from patients with histologically documented AML undergoing routine diagnostic procedures with Virginia Commonwealth University IRB approval (#HM 12517). Primary AML samples (blasts > 70% and viability > 95%) and normal human cord blood (CB) $CD34^+$ cells were isolated as described earlier (12). Patient clinical, molecular, and cytogenetic characteristics are reported in Supplemental Table S1.

The selective Chk1 inhibitor AZD1775 and the pan-HDAC inhibitor Vorinostat (formerly SAHA) were provided by AstraZeneca (Wilmington, DE) and Merck (Whitehouse Station, N.J.) through National Cancer Institute, NIH. SBHA was purchased from Calbiochem. Reagents were formulated in DMSO and stored at −20°C. Final DMSO concentrations were < 0.1%.

Next-generation sequencing (NGS) of primary AML samples

Primary AML samples (mononuclear cells) were analyzed by NGS using the Ion AmpliSeq™ Cancer Hotspot Panel v2, which surveys hotspot regions of 50 oncogenes and tumor suppressor genes. NGS analyses were conducted using the Ion Torrent™ targeted sequencing technology (Life Technologies, Grand Island, NY).

Analysis of cell cycle and checkpoints

Cell cycle analysis by propidium iodide (PI) staining in the presence of RNase A was performed by flow cytometry (FCM) using Modfit LT2.0 software (Topsham, ME) as described previously (12).

Premature mitotic entry was assessed as reported earlier (22). Cells were fixed in ice-cold 70% ethanol and permeabilized with 0.25% Triton X-100 in PBS, followed by staining with AlexaFluor 488-conjugated anti-phospho-histone H3 (p-H3, S10) antibody (Cell Signaling, Beverly, MA) at 4°C in dark. After PI staining for cell cycle analysis as above, the percentage and cell cycle distribution of p-H3-positive cells was determined by FCM.

For G1/S and intra-S phase checkpoint assessment, the Click-iT™ EdU CellCycle 488-Red (7-AAD) Assay Kit (Invitrogen) was used to monitor DNA replication through incorporation of the thymidine analogue 5-ethynyl 2-deoxyuridine (EdU, 10 μM, 30 min) into genomic DNA during DNA synthesis by FCM (12).

To monitor DNA replication and mitotic entry simultaneously, cells were labeled with EdU, followed by staining for p-H3 as above.

Immunofluorescence

Cytospin slides were fixed in 4% paraformaldehyde for 1 h, permeabilized in 0.25% Triton X-100 in PBS, blocked in 1% BSA and 2% FBS in PBS, followed by staining with AlexaFluor 488-conjugated anti-p-H3 antibody (22). Slides were mounted using Vectashield containing DAPI. Images were captured using a Zeiss LSM 700 confocal microscope or Olympus IX71 Research Inverted System Microscope with a DP73;17MP Color Camera.

For double staining for EdU and p-H3, cytospin slides were prepared after pulse labeling with EdU, followed by immunofluorescence staining for p-H3 using secondary AlexaFluor 594-conjugated antibody (Cell Signaling).

Analysis of cell death, RNA interference, and Western blot analysis

(See Supplemental Methods).

Animal studies

Animal studies approved the VCU IACUC, were performed in accordance with the U.S. Department of Agriculture and Department of Health and Human Services, and the NIH. NOD/SCID-gamma mice (Jackson Laboratories) were subcutaneously inoculated in the flank with 5×10^6 luciferase-labeled U937 cells. After luciferase activity was detected, AZD1775 and Vorinostat were administrated by oral gavage (p.o.) or intraperitoneal (i.p.) injection, respectively. Control animals received equal volumes of vehicle. Mice were monitored every other day after luciferin i.p. injection using an IVIS 200 imaging system (Xenogen Corporation, Alameda, CA). Tumor size was measured by caliper and volumes calculated using the formula $(L \times W^2)/2$, with L = length and W = width. Body weights were measured every other day throughout the study. When tumor size reached 2,000 mm^3 or other humane endpoints (e.g., abscessed or necrotic tumors) reached, mice were euthanized in accordance with institutional guidelines.

Statistical analysis

Values represent the means ± SD for at least three independent experiments performed in triplicate. Significance of differences between experimental variables was determined using the Student's t test or One-way ANOVA with Tukey-Kramer Multiple Comparisons Test (two-sided). The significance of *P* values was < 0.05 (*) and < 0.01 (**) wherever indicated. Analysis of synergism was performed by Median Dose Effect analysis using Calcusyn software (Biosoft, Ferguson, MO). Kaplan-Meier survival analysis utilized IBM SPSS Statistics software.

RESULTS

AZD1775/HDACI co-administration reduces total and phosphorylated Wee1 and diminishes cdc2/Cdk1 Y15 phosphorylation in AML cells

Exposure (24 h) to AZD1775 (100–500 nM) modestly reduced Wee1 phosphorylation on S642, an event occurring during S and G2 phases and required for 14-3-3 binding (23), in various leukemia cells, including p53-null or -mutant U937 (Fig 1a) and MV-4-11 (FLT-ITD, Fig 1b), as well as p53-wild-type (wt) MOLM-13 (FLT3-ITD, Fig 1c) and OCI-AML3 (Fig 1d). The HDACIs Vorinostat or SBHA also modestly reduced S624 phosphorylation in certain cell lines (e.g., MV-4-11 and OCI-AML3). However, combined treatment profoundly diminished S462 phosphorylation of Wee1 in all lines. Whereas AZD1775 or HDACIs alone had little effect, AZD1775/HDACI co-administration also reduced total Wee1 protein (Fig 1a–d). Y15 phosphorylation of cdc2/Cdk1, a biomarker of Wee1 kinase activity (24, 25), was then examined. AZD1775 by itself diminished cdc2/Cdk1 Y15 phosphorylation, and this effect was modestly but discernibly enhanced by HDACIs, although protein levels were unaffected (Fig 1a–d). Notably, diminished cdc2/Cdk1 Y15 phosphorylation with combined treatment was observed as early as 8 h after drug administration (Supplemental Fig S1A). Thus, AZD1775 inactivates Wee1 in both p53 wt and mutant leukemia cells, an event enhanced by HDACIs and accompanied by pronounced cdc2/Cdk1 Y15 dephosphorylation.

AZD1775 interacts synergistically with HDACIs in AML cells carrying mutant p53 or FLT3-ITD

Whereas p53 loss or mutation is relatively uncommon in AML (e.g., 5 – 10%) (26) compared to FLT3 mutations (e.g., 27%) (2), they occur more commonly in therapy-related AML (t-AML; e.g., 40% to 50%) (27), and are associated with poor prognosis (26). Effects of AZD1775 and HDACIs were evaluated in p53-null cells (U937) (12) or cells with p53 point mutations at codon 344 (MV4-11, which also expresses FLT3-ITD) (12). Notably, co-administration (24 h) of marginally toxic AZD1775 concentrations (e.g., 50–750 nM) with minimally toxic and clinically relevant concentrations of Vorinostat (e.g., 0.5–1.5 μM) strikingly induced apoptosis in both U937 (Fig 2a and Supplemental Fig S1B) and MV4-11 cells (Fig 2b and Supplemental Fig S1C). Similar results were obtained with another HDACI (SBHA; 5–20 μM). Time course studies demonstrated that AZD1775/Vorinostat-induced apoptosis occurred at 16 h and increased further over the ensuing 48 h in U937 cells (Supplemental Fig S1D). Sequential HDACI pre-treatment (24 h) followed by AZD1775 also markedly increased apoptosis, comparable to simultaneous administrations, whereas the reverse sequence was less effective (data not shown).

Co-administration of AZD1775 and either Vorinostat (Fig 2c) or SBHA (Supplemental Fig S1E) markedly increased caspase-9 cleavage/activation and PARP degradation in U937 and MV4-11 cells, associated with significant reductions in colony formation (Fig 2d). Finally, isobologram analysis yielded CI values < 1.0 in both cell lines, indicating synergism (Fig 2e). Together, these findings suggest that targeting Wee1 by AZD1775 sharply potentiates HDACI lethality in p53-mutant AML cells, including those expressing FLT3-ITD.

The AZD1775/HDACI regimen is highly active in AML cells expressing wild type p53

Responses to Wee1 inhibitors, particularly when combined with DNA damaging agents (28) or radiation (29), is enhanced in p53-deficient tumor cells, presumably due to reliance on the G2/M checkpoint when the G1/S checkpoint is impaired (21). Parallel studies were therefore performed in leukemia cells expressing wt p53, including OCI-AML3 (12) and MOLM-13 (which also expresses FLT3-ITD)(12) cells. Notably, p53-wt leukemia cells exhibited equivalent sensitivity to the AZD1775/HDACI regimen (Fig 3a and 3b), compared to p53-deficient U937 and MV4-11 cells (Supplemental Fig S1B–C). Isobologram analysis also revealed synergism (i.e., CI values < 1.0) in AML-3 cells and MOLM-13 cells (Fig 3c). Significantly, co-administration of HDACIs (e.g., Vorinostat or SBHA) markedly increased caspase 9 cleavage/activation and PARP degradation (Fig 3d), in p53 wt leukemia cells. Collectively, these findings indicate that, in contrast to settings in which AZD1775 potentiates genotoxic agent and radiation activity primarily in p53-deficient tumors (28, 29), the AZD1775/HDACI regimen is effective in both p53-mutant and -wt leukemias.

HDACIs abrogate AZD1775-induced Chk1 activation and cdc2/Cdk1 T14 phosphorylation, accompanied by premature mitotic entry and DNA damage

AZD1775 ± HDACI effects on activation of Chk1, a key regulator of multiple cell cycle checkpoints as well as DNA replication and repair (13), was then examined. Notably, AZD1775 sharply increased Chk1 phosphorylation on three serine residues (S296, S317, and S345), essential for Chk1 activation (30), in p53-deficient U937 (Fig 4a) and MV4-11 (Fig 4b), as well as p53-wt MOLM-13 cells (Fig 4c). Consistent with this finding, AZD1775 also induced, in sharp contrast to Y15 dephosphorylation, cdc2/Cdk1 T14 phosphorylation (Fig 4d–f), an event primarily mediated by another Wee family member, Myt1 (31). Significantly, AZD1775 did not induce Myt1 activation (e.g., S83 phosphorylation; Supplemental Fig S2A), arguing against the possibility that increased T14 phosphorylation primarily stems from Myt1 activation. Importantly, either Vorinostat (Fig 4a–c) or SBHA (Fig 4c and Supplemental Fig S2B–C) administration essentially abrogated AZD1775-induced Chk1 phosphorylation/activation, in part through Chk1 down-regulation, as well as inhibitory T14 phosphorylation of cdc2/Cdk1. Moreover, AZD1775/HDACI co-treatment sharply increased S10 phosphorylation of histone H3, a premature mitotic entry indicator (21), associated with a pronounced increase in DNA damage, manifested by expression of the double-strand break (DSB) indicator γH2A.X (32) in both p53-deficient (e.g., U937 [Fig 4d and Supplemental Fig S2B] and MV4-11 [Fig 4e and Supplemental Fig S2C]) and p53-wt cells (e.g., MOLM-13 [Fig 4f] and OCI-AML3 [Supplemental Fig S2D]). Of note, reversal of both AZD1775-mediated Chk1 activation and cdc2/Cdk1 T14 phosphorylation by Vorinostat, accompanied by increased γH2A.X expression, occurred at an early interval (e.g., 8 h; Supplemental Fig S1A), considerably prior to obvious apoptosis induction (i.e., 16 h Supplementary Fig S1D), arguing that the former is unlikely to be a secondary event. These findings raise the possibility that Chk1 activation and cdc2/Cdk1 T14 phosphorylation represent compensatory responses to Wee1 inhibition, and that HDACIs disrupt these events, triggering premature mitotic entry, DNA damage, and cell death in both p53-wt and -deficient AML cells.

Combined Wee1/HDAC inhibition triggers mitotic lethality and abrogates the G1/S checkpoint

Effects on cell cycle checkpoints were then examined, using the mitotic inhibitor Taxol as a control. Cell cycle analysis of U937 cells revealed that while HDACIs increased the G2/M sub-population (33), this event was enhanced by AZD1775 as early as 8 h after drug treatment (Fig 5a, top, and Supplemental Fig S3A). Notably, whereas both AZD1775 and HDACIs alone modestly increased the mitotic index (MI) at 8 h, reflected by positivity of S10 phosphorylated histone H3 (p-H3), combined exposure strikingly increased the p-H3 MI (e.g., 3.4- and 3.7- fold increases for AZD1775/Vorinostat or /SBHA, respectively; Fig 5a, bottom), consistent with premature mitotic entry at this early interval. However, while AZD1775 ± HDACIs clearly decreased S-phase cells, neither agent alone or in combination obviously affected DNA replication, manifested by a minimal increase in EdU-positive cells at 8 h (Supplemental Fig S3B–C). Interestingly, AZD1775/Vorinostat or /SBHA co-treatment for 16 h sharply arrested cells in early S-phase (Fig 5b, top, and Supplemental Fig S4A) and increased newly replicated DNA incorporating EdU (34) (Fig 5b, bottom, and Supplemental Fig S4B), accompanied by persistent increases in premature mitotic entry (e.g., increased p-H3 MI; Fig 5b, bottom, and Supplemental Fig S4C). Fluorescence microscopy demonstrated robust increases in both p-H3- and EdU-positive cells after 16-h co-exposure to AZD1775 and Vorinostat or SBHA (Fig 5c and Supplemental Fig S4D). Furthermore, confocal microscopy of AZD1775/HDACI-treated cells (16 h) revealed markedly aberrant mitosis characterized by multiple mitotic abnormalities e.g., anaphase bridging, mono- or multi-polar spindles, centrosome clustering, etc. in p-H3-positive cells (22, 35) (Fig 5d). Such findings indicate that AZD1775/HDACI co-treatment induces premature mitotic entry, aberrant mitosis, and accumulation of early S phase cells with increased *de novo* DNA replication, and suggest that Wee1 and HDAC inhibitors interact reciprocally to disrupt both G2/M and G1/S checkpoints.

Wee1 shRNA knock-down significantly increases AML cell susceptibility to HDACIs, associated with premature mitotic entry

To validate the functional significance of Wee1 inhibition on HDACI responses in leukemic cells, U937 Wee1 shRNA cells were employed (Fig 6a, inset; two clones designated D3 and E3). Notably, Wee1 knock-down significantly sensitized cells to SBHA- and Vorinostat-induced apoptosis, compared to scrambled sequence controls (shNC; Fig 6a, $P < 0.01$ or 0.05 in all cases). In contrast to AZD1775, stable Wee1 knock-down did not discernibly affect cdc2/Cdk1 Y15 phosphorylation; however, Vorinostat or SBHA markedly reduced this inhibitory phosphorylation in Wee1 knock-down cells (Fig 6b), like AZD1775 co-treatment (Fig 1a). This was accompanied by sharply increased histone H3 S10 phosphorylation, indicating premature mitotic entry, pronounced γH2A.X induction, and increased PARP cleavage (Fig 6c). These findings argue that Wee1 inhibition plays a significant functional role in AZD1775/HDACI interactions in leukemia cells.

The AZD1775/HDACI regimen is active against primary AML blasts carrying various genetic aberrations and leukemia-initiating cells (LIC)-enriched populations, but not normal hematopoietic cells

Parallel studies were performed in bulk populations of 6 primary AML samples (all ≥ 70% blasts). In a representative study, AZD1775 alone had little effect, while Vorinostat (Fig 7a, top) or SBHA (Supplemental Fig S5A, bottom) exhibited modest activity towards AML blasts. However, AZD1775/HDACI co-exposure markedly increased Annexin V-positive (apoptotic) cells (e.g., ≥ 50–60%). Assessment of mitochondrial membrane potential ($\Delta\Psi m$) loss (reduced $DiOC_6$ uptake) and cell death ($7\text{-}AAD^+$) confirmed enhanced lethality in 5 of total 6 tested primary AML samples, while only one sample (patient #6) weakly displayed a loss of cell viability (Supplemental Fig S6). These results were expressed as median responses in Fig 7b ($P < 0.01$ for the combination vs each agent alone). Additionally, genetic mutations were analyzed by NGS in five samples (Fig 7c), of which the four responding samples (patients #1–4) each carried four or five somatic mutations, including p53, FLT3, NRAS, KRAS, BRAF, PDGFRA, MET, STK11, SMARCB1, or APC. Notably, in these samples, patient #1 and #2 expressed wt p53, while #3 and #4 carried p53 mutations. Moreover, FLT3 mutations were found in 2/4 responding samples (patients #2 and #4). However, the modestly-responding sample (patient #6) exhibited only the favorable prognosis NPM1 mutation. These results argue that the AZD1775/HDACI regimen may be active against primary leukemia cells expressing either wt or mutant p53, as in leukemia cell lines.

Regimen activity was then examined in the primary AML $CD34^+/CD38^-/CD123^+$ sub-population enriched for leukemia-initiating cells (19, 36) using multicolor FCM. Whereas AZD1775 had moderate effects, HDACIs alone exhibited clear lethality. However, combined AZD1775/Vorinostat (Fig 7d) or /SBHA treatment (Supplemental Fig S5B) sharply increased the percentage of Annexin V-positive (apoptotic) cells (e.g., > 60–70%). Similar results were obtained in two additional primary AML samples (data not shown). In contrast, identical regimens exhibited minimal toxicity toward normal cord blood $CD34^+$ cells (Fig 7a, bottom, and Supplemental Fig S5A, bottom). Finally, as in leukemia cell lines, combined AZD1775/HDACI treatment of primary AML blasts also induced pronounced DNA damage (e.g., γH2A.X expression) and apoptosis (e.g., PARP degradation; Fig 7e). Together, these findings indicate that the ability of AZD1775 to promote HDACI lethality can occur independently of p53 status in primary AML blasts, including those bearing poor-prognostic mutations, and also raise the possibility that this regimen targets primitive AML progenitors while sparing normal hematopoietic cells.

AZD1775/Vorinostat reduces tumor burden and prolongs survival in an AML xenograft model

NOD/SCID-gamma mice were inoculated in the right flank with luciferase-expressing U937 cells; once tumors were visible, mice were treated with Vorinostat (100 mg/kg) ± AZD1775 (50 mg/kg). Combined treatment significantly reduced tumor volume (Fig 8a, $P < 0.05$ vs vehicle or individual treatment) and luciferase signals compared to single-agent treatment (Fig 8b). Representative photographs confirmed marked tumor size reduction following combined treatment (Fig 8c). Moreover, combined treatment significantly prolonged animal

survival by Kaplan Meier analysis (e.g., median survival of ≥ 40 days, compared to 31.5 or 30 days for AZD1775 or Vorinostat alone respectively, $P < 0.05$; Fig 8d). Notably, 3/5 mice in the combination group were sacrificed because of humane endpoints (e.g. abscessed or necrotic tumors), rather than tumor size ≥ 2,000 mm^3. During the entire study, mice did not display significant body weight loss (i.e., ≥ 10% of initial weight; Supplemental Fig S7) or other signs of toxicity. Finally, Western blot analysis of tumor lysates revealed that combined AZD1775/Vorinostat treatment clearly reduced Wee1 S642 and CDK1 Y15 and T14 phosphorylation, accompanied by increased γH2A.X expression and PARP cleavage (Fig 8e). Together, these findings argue that AZD1775 potentiates HDACI anti-leukemic activity *in vivo* as well as *in vitro*, potentially through similar mechanisms.

DISCUSSION

DDR deregulation in neoplastic cells has prompted therapeutic efforts to disrupt DNA damage checkpoints to potentiate genotoxic agent lethality (13), leading to the development of agents targeting Chk1 (13), ATM (37), ATR (38), and most recently Wee1(21). As Wee1 plays a critical role in the G2/M DNA damage checkpoint (28), Wee1 inhibitors such as AZD1775 have been employed to improve the efficacy of DNA damaging chemotherapeutic agents and ionizing radiation through mitotic lethality (21), primarily in solid tumor malignancies (25, 39–45). This strategy is based on pre-clinical reports that AZD1775 potentiates genotoxic agent (28) and ionizing radiation (29) activity, particularly in p53-deficient tumors, through mitotic lethality (21). Wee1 also plays critical roles in S-phase DNA replication (e.g., replication fork stabilization) (18, 46), cell division timing (47), and DNA repair (e.g., HR) (48). Recently, Wee1 has been identified as an AML target, and potentiation of ara-C or mTOR inhibitor lethality by Wee1 inhibition has been reported in such cells (19, 20, 49). Furthermore, perturbations in cell cycle-regulatory genes (including Cdks, cyclins, and Cdk endogenous inhibitors) are frequent in AML (e.g., 66%) and correlate with poor prognosis (50). Additionally, aberrations of genes related to checkpoints (e.g., ATM, ATR, Chk1, Chk2, Wee1) or DNA repair (e.g., RAD51, BRCA1, BRCA2, MLH1 etc.) occur in 41% of AML patients (50). In this context, HDACI mechanisms of action (MOAs) have also focused on DNA damage induction through disruption of DNA damage checkpoints and/or repair (8). However, information concerning Wee1/HDAC inhibitor interactions is lacking in AML or other tumor types. Together, these considerations provide a rationale for exploring Wee1/HDAC inhibition in AML.

Wee1 inhibitor MOAs initially focused on disruption of the G2/M checkpoint, which permits cells to repair genotoxic agent-mediated DNA damage before entry into mitosis for cell division (28). G2/M checkpoint abrogation triggers premature mitotic entry, and mitotic catastrophe (28, 51). However, the role of Wee1 in the S phase checkpoint (52), which ensures proper DNA replication (46), represents an additional mechanism by which Wee1 inhibitors promote cell death. HDACIs have also been reported to disrupt both G2/M and S-phase checkpoints (8). Notably, HDACI co-administration with AZD1775 enhanced Wee1 inactivation/down-regulation and cdc2/Cdk1 Y15 dephosphorylation (activation), which when unscheduled, triggers cell death (53). Consistent with these actions, Wee1/HDACI co-exposure also induced premature mitotic entry, reflected by marked increases in histone H3 S10 phosphorylation and the p-H3 mitotic index (22), due to disruption of the G2/M

checkpoint (54). Significantly, these events occurred at early intervals (e.g., 8 h) prior to apoptosis induction (e.g., 16 h), and persisted over 24 h. Moreover, Wee1 knock-down also sharply increased HDACI lethality in association with similar events (e.g., enhanced cdc2/Cdk1 Y15 dephosphorylation and DNA damage). Interestingly, combined treatment also increased early S phase accumulation and newly replicated DNA (i.e., EdU incorporation) at relatively late intervals (e.g., 16 h), suggesting abrogation of the G1/S-phase checkpoint which prevents S-phase entry (i.e., the G1/S transition) in the presence of DNA damage through inhibition of DNA replication initiation (13). Finally, markedly aberrant mitoses (e.g., monopolar or multipolar spindles, anaphase bridging, centrosome clustering, etc.) were observed in co-treated cells, accompanied by robust DNA damage and cell death. Together, these findings argue that whereas Wee1 inhibition alone (55, 56) or in combination with genotoxic agents (25, 39, 41) disrupts the G2/M checkpoint, Wee1 and HDAC inhibitors interact reciprocally to disrupt both the G1/S and G2/M checkpoints. However, inasmuch as HDACIs disrupt multiple events of the DDR (9, 10), including down-regulation of Chk1 (11, 12) as well as DNA repair proteins (14), the possibility that additional mechanism(s) implicated in the DDR might also contribute to synergism between HDAC and Wee1 inhibitors cannot be excluded. It is also possible that increased lethality (particularly in primary AML samples) in the present setting may not exclusively reflect apoptosis, but may also stem from alternative forms of cell death.

Several lines of evidence suggest that that Wee1/HDAC inhibitor synergism involves Chk1. While both Chk1 and Wee1 are involved in the G2/M checkpoint (30), they share other, unrelated functions i.e., stabilization of replication forks and multiple mitotic events (21, 57). Moreover, Chk1 phosphorylates and activates Wee1 (13, 58). In this regard, recent studies have demonstrated that combining Wee1 inhibitors (e.g., AZD1775) with Chk1 inhibitors induces pronounced DNA damage (e.g., increased γH2A.X levels) and apoptosis (22, 45, 59), including in AML cells (60). Such interactions have been related to the role of Chk1 in the G1/S checkpoint (13) or forced mitotic entry of S phase cells (22). Interestingly, Chk1 inhibition also promotes HDACI-mediated DNA damage and lethality in AML cells (12). Consistent with earlier observations (56, 60), AZD1775 clearly triggered Chk1 activation (e.g., phosphorylation on all three critical activation sites including S296, S317, and S345) (30). Of note, this event was accompanied by cdc2/Cdk1 phosphorylation on the inhibitory site T14. Whereas Wee1 primarily phosphorylates cdc2/Cdk1 Y15, T14 is preferentially phosphorylated by Myt1 (31). However, failure of AZD1775 to activate Myt1 suggests, albeit indirectly, that T14 phosphorylation stems from Chk1 activation through inhibition/degradation of Cdc25, a phosphatase that dephosphorylates cdc2/Cdk1 T14 and Y15 sites (30). Collectively, these findings suggest that AZD1775-induced Chk1 activation, leading to cdc2/Cdk1 T14 phosphorylation, represents a compensatory response to Wee1 disruption that limits cdc2/Cdk1 activation and checkpoint abrogation. However, HDACIs not only enhanced Wee1 inhibition and Y15 dephosphorylation, they also sharply attenuated AZD1775-mediated T14 phosphorylation, presumably through down-regulation/inactivation of Chk1 (11, 12). As a consequence, AZD1775/HDACI co-administration resulted in cdc2/Cdk1 dephosphorylation on both inhibitory Y15 and T14 sites, triggering full (and “inappropriate”) activation, thereby abrogating both G1/S and G2/M checkpoints and potentiating apoptosis (53). Indeed, the early (e.g., 8 h) T14 and Y15 dephosphorylation of

cdc2/Cdk1 was accompanied by premature mitotic entry and G1/S checkpoint abrogation in cells co-exposed to AZD1775 and HDACIs. Thus, HDACIs, in addition to disrupting DNA repair (14), may recapitulate Chk1 inhibitor actions in promoting Wee1 inhibitor lethality (22).

Although p53 mutations occur relatively rarely in *de novo* AML, they are more common in relapsed/refractory disease and are associated with poor prognosis (26). In previous studies involving solid tumors, AZD1775 principally potentiated the lethality of genotoxic agents (e.g., gemcitabine, 5-FU) (25, 41) or radiation (40) in p53-deficient cells. Of note, AZD1775 potentiates Ara-C lethality in both p53-wt and -deficient AML cell lines (19). Consistent with the latter findings, AZD1775 enhanced HDACI lethality in p53-wt or -deficient leukemia cells to a roughly equivalent extent, as well as in primary AML blasts expressing either wt or mutant p53. Significantly, similar interactions occurred in leukemia cell lines expressing FLT3-ITD, which may reflect intrinsic homologous recombination (HR) repair defects (15). as well as primary AML cells bearing FLT3 mutations, Collectively, these findings suggest that the Wee1/HDAC inhibitor strategy acts independently of p53 status and is effective against cells expressing mutant FLT3, a poor-prognostic marker in AML.

In summary, the present findings indicate that genetic or pharmacologic interruption of Wee1 function sharply potentiates the anti-leukemic activity of clinically relevant HDACIs (e.g., Vorinostat) independently of p53 status, and argue that this interaction involves interference with both the G1/S and G2/M checkpoints, leading to robust induction of DNA damage, mitotic disruption, and apoptosis. Significantly, similar interactions occur in primary AML blasts and primitive (i.e., $CD34^{+}/CD38^{-}/CD123^{+}$) progenitors, including those bearing multiple poor-prognostic genetic mutations (e.g., p53, FLT3), but not in normal hematopoietic cells. Importantly, *in vivo* administration of these agents was well tolerated and markedly reduced tumor burden and increased survival *in vivo*. While pre-clinical studies justify ongoing initiatives employing Wee1 inhibitors to improve the activity of standard genotoxic agents in solid tumors (e.g., http://clinicaltrials.gov/show/NCT02151292; http://clinicaltrials.gov/show/NCT02087176), the present findings provide a foundation for combining Wee1 inhibitors (e.g., AZD1775) with HDACIs in hematopoietic malignancies such as AML. Accordingly, efforts to develop this strategy are currently underway.

Supplementary Material

Refer to Web version on PubMed Central for supplementary material.

Acknowledgments

This work was supported by the National Institutes of Health [Grant CA93738] and the Leukemia and Lymphoma Society of America [Grant R6238]. Plasmid preparation was performed at the VCU Macromolecule Core Facility, supported, in part, with funding from NIH-NCI Cancer Center Core Grant 5P30CA016059-29; Confocal microscopies were performed at the VCU Department of Anatomy and Neurobiology Microscopy Facility, supported, in part, with funding from NIH-NINDS Center Core Grant 5P30NS047463.

References

1. Welch JS, Ley TJ, Link DC, Miller CA, Larson DE, Koboldt DC, et al. The origin and evolution of mutations in acute myeloid leukemia. Cell. 2012 Jul 20; 150(2):264–78. [PubMed: 22817890]
2. Levis M. FLT3 mutations in acute myeloid leukemia: what is the best approach in 2013? Hematology Am Soc Hematol Educ Program. 2013; 2013:220–6. [PubMed: 24319184]
3. Roboz GJ, Rosenblat T, Arellano M, Gobbi M, Altman JK, Montesinos P, et al. International Randomized Phase III Study of Elacytarabine Versus Investigator Choice in Patients With Relapsed/Refractory Acute Myeloid Leukemia. J Clin Oncol. 2014 Jun 20; 32(18):1919–26. [PubMed: 24841975]
4. Grant S, Dai Y. Histone deacetylase inhibitors and rational combination therapies. Adv Cancer Res. 2012; 116:199–237. [PubMed: 23088872]
5. Bots M, Verbrugge I, Martin BP, Salmon JM, Ghisi M, Baker A, et al. Differentiation therapy for the treatment of t(8;21) acute myeloid leukemia using histone deacetylase inhibitors. Blood. 2014 Feb 27; 123(9):1341–52. [PubMed: 24415537]
6. Bose P, Grant S. Orphan drug designation for pracinostat, volasertib and alvocidib in AML. Leuk Res. 2014 Jun 17.
7. Grant S, Easley C, Kirkpatrick P. Vorinostat. Nat Rev Drug Discov. 2007 Jan; 6(1):21–2. [PubMed: 17269160]
8. Bose P, Dai Y, Grant S. Histone deacetylase inhibitor (HDACI) mechanisms of action: Emerging insights. Pharmacol Ther. 2014 Apr 24.
9. Lee JH, Choy ML, Ngo L, Foster SS, Marks PA. Histone deacetylase inhibitor induces DNA damage, which normal but not transformed cells can repair. Proc Natl Acad Sci U S A. 2010 Aug 17; 107(33):14639–44. [PubMed: 20679231]
10. Koprinarova M, Botev P, Russev G. Histone deacetylase inhibitor sodium butyrate enhances cellular radiosensitivity by inhibiting both DNA nonhomologous end joining and homologous recombination. DNA Repair (Amst). 2011 Sep 5; 10(9):970–7. [PubMed: 21824827]
11. Brazelle W, Kreahling JM, Gemmer J, Ma Y, Cress WD, Haura E, et al. Histone deacetylase inhibitors downregulate checkpoint kinase 1 expression to induce cell death in non-small cell lung cancer cells. PLoS One. 2010; 5(12):e14335. [PubMed: 21179472]
12. Dai Y, Chen S, Kmieciak M, Zhou L, Lin H, Pei XY, et al. The novel Chk1 inhibitor MK-8776 sensitizes human leukemia cells to HDAC inhibitors by targeting the intra-S checkpoint and DNA replication and repair. Mol Cancer Ther. 2013 Jun; 12(6):878–89. [PubMed: 23536721]
13. Dai Y, Grant S. New insights into checkpoint kinase 1 in the DNA damage response signaling network. Clin Cancer Res. 2010 Jan 15; 16(2):376–83. [PubMed: 20068082]
14. Kachhap SK, Rosmus N, Collis SJ, Kortenhorst MS, Wissing MD, Hedayati M, et al. Downregulation of homologous recombination DNA repair genes by HDAC inhibition in prostate cancer is mediated through the E2F1 transcription factor. PLoS One. 2010; 5(6):e11208. [PubMed: 20585447]
15. Fan J, Li L, Small D, Rassool F. Cells expressing FLT3/ITD mutations exhibit elevated repair errors generated through alternative NHEJ pathways: implications for genomic instability and therapy. Blood. 2010 Dec 9; 116(24):5298–305. [PubMed: 20807885]
16. Petruccelli LA, Pettersson F, Del Rincon SV, Guilbert C, Licht JD, Miller WH Jr. Expression of leukemia-associated fusion proteins increases sensitivity to histone deacetylase inhibitor-induced DNA damage and apoptosis. Mol Cancer Ther. 2013 Aug; 12(8):1591–604. [PubMed: 23536727]
17. Gaymes TJ, Padua RA, Pla M, Orr S, Omidvar N, Chomienne C, et al. Histone deacetylase inhibitors (HDI) cause DNA damage in leukemia cells: a mechanism for leukemia-specific HDI-dependent apoptosis? Mol Cancer Res. 2006 Aug; 4(8):563–73. [PubMed: 16877702]
18. Sorensen CS, Syljuasen RG. Safeguarding genome integrity: the checkpoint kinases ATR, CHK1 and WEE1 restrain CDK activity during normal DNA replication. Nucleic Acids Res. 2012 Jan; 40(2):477–86. [PubMed: 21937510]
19. Porter CC, Kim J, Fosmire S, Gearheart CM, van LA, Baturin D, et al. Integrated genomic analyses identify WEE1 as a critical mediator of cell fate and a novel therapeutic target in acute myeloid leukemia. Leukemia. 2012 Jun; 26(6):1266–76. [PubMed: 22289989]

20. Tibes R, Bogenberger JM, Chaudhuri L, Hagelstrom RT, Chow D, Buechel ME, et al. RNAi screening of the kinome with cytarabine in leukemias. Blood. 2012 Mar 22; 119(12):2863–72. [PubMed: 22267604]
21. Do K, Doroshow JH, Kummar S. Wee1 kinase as a target for cancer therapy. Cell Cycle. 2013 Oct 1; 12(19):3159–64. [PubMed: 24013427]
22. Aarts M, Sharpe R, Garcia-Murillas I, Gevensleben H, Hurd MS, Shumway SD, et al. Forced mitotic entry of S-phase cells as a therapeutic strategy induced by inhibition of WEE1. Cancer Discov. 2012 Jun; 2(6):524–39. [PubMed: 22628408]
23. Katayama K, Fujita N, Tsuruo T. Akt/protein kinase B-dependent phosphorylation and inactivation of WEE1Hu promote cell cycle progression at G2/M transition. Mol Cell Biol. 2005 Jul; 25(13): 5725–37. [PubMed: 15964826]
24. Mizuarai S, Yamanaka K, Itadani H, Arai T, Nishibata T, Hirai H, et al. Discovery of gene expression-based pharmacodynamic biomarker for a p53 context-specific anti-tumor drug Wee1 inhibitor. Mol Cancer. 2009; 8:34. [PubMed: 19500427]
25. Hirai H, Iwasawa Y, Okada M, Arai T, Nishibata T, Kobayashi M, et al. Small-molecule inhibition of Wee1 kinase by MK-1775 selectively sensitizes p53-deficient tumor cells to DNA-damaging agents. Mol Cancer Ther. 2009 Nov; 8(11):2992–3000. [PubMed: 19887545]
26. Wattel E, Preudhomme C, Hecquet B, Vanrumbeke M, Quesnel B, Dervite I, et al. p53 mutations are associated with resistance to chemotherapy and short survival in hematologic malignancies. Blood. 1994 Nov 1; 84(9):3148–57. [PubMed: 7949187]
27. Christiansen DH, Andersen MK, Pedersen-Bjergaard J. Mutations with loss of heterozygosity of p53 are common in therapy-related myelodysplasia and acute myeloid leukemia after exposure to alkylating agents and significantly associated with deletion or loss of 5q, a complex karyotype, and a poor prognosis. J Clin Oncol. 2001 Mar 1; 19(5):1405–13. [PubMed: 11230485]
28. De Witt Hamer PC, Mir SE, Noske D, Van Noorden CJ, Wurdinger T. WEE1 kinase targeting combined with DNA-damaging cancer therapy catalyzes mitotic catastrophe. Clin Cancer Res. 2011 Jul 1; 17(13):4200–7. [PubMed: 21562035]
29. Mir SE, De Witt Hamer PC, Krawczyk PM, Balaj L, Claes A, Niers JM, et al. In silico analysis of kinase expression identifies WEE1 as a gatekeeper against mitotic catastrophe in glioblastoma. Cancer Cell. 2010 Sep 14; 18(3):244–57. [PubMed: 20832752]
30. Smith J, Tho LM, Xu N, Gillespie DA. The ATM-Chk2 and ATR-Chk1 pathways in DNA damage signaling and cancer. Adv Cancer Res. 2010; 108:73–112. [PubMed: 21034966]
31. Booher RN, Holman PS, Fattaey A. Human Myt1 is a cell cycle-regulated kinase that inhibits Cdc2 but not Cdk2 activity. J Biol Chem. 1997 Aug 29; 272(35):22300–6. [PubMed: 9268380]
32. Darzynkiewicz Z, Traganos F, Zhao H, Halicka HD, Skommer J, Wlodkowic D. Analysis of individual molecular events of DNA damage response by flow- and image-assisted cytometry. Methods Cell Biol. 2011; 103:115–47. [PubMed: 21722802]
33. Hirose T, Sowa Y, Takahashi S, Saito S, Yasuda C, Shindo N, et al. p53-independent induction of Gadd45 by histone deacetylase inhibitor: coordinate regulation by transcription factors Oct-1 and NF-Y. Oncogene. 2003 Oct 30; 22(49):7762–73. [PubMed: 14586402]
34. Hansen RS, Thomas S, Sandstrom R, Canfield TK, Thurman RE, Weaver M, et al. Sequencing newly replicated DNA reveals widespread plasticity in human replication timing. Proc Natl Acad Sci U S A. 2010 Jan 5; 107(1):139–44. [PubMed: 19966280]
35. Eriksson D, Lofroth PO, Johansson L, Riklund KA, Stigbrand T. Cell cycle disturbances and mitotic catastrophes in HeLa Hep2 cells following 2.5 to 10 Gy of ionizing radiation. Clin Cancer Res. 2007 Sep 15; 13(18 Pt 2):5501s–8s. [PubMed: 17875782]
36. Jordan CT, Upchurch D, Szilvassy SJ, Guzman ML, Howard DS, Pettigrew AL, et al. The interleukin-3 receptor alpha chain is a unique marker for human acute myelogenous leukemia stem cells. Leukemia. 2000 Oct; 14(10):1777–84. [PubMed: 11021753]
37. Batey MA, Zhao Y, Kyle S, Richardson C, Slade A, Martin NM, et al. Preclinical evaluation of a novel ATM inhibitor, KU59403, in vitro and in vivo in p53 functional and dysfunctional models of human cancer. Mol Cancer Ther. 2013 Jun; 12(6):959–67. [PubMed: 23512991]

38. Reaper PM, Griffiths MR, Long JM, Charrier JD, Maccormick S, Charlton PA, et al. Selective killing of ATM- or p53-deficient cancer cells through inhibition of ATR. Nat Chem Biol. 2011 Jul; 7(7):428–30. [PubMed: 21490603]
39. Kreahling JM, Foroutan P, Reed D, Martinez G, Razabdouski T, Bui MM, et al. Wee1 inhibition by MK-1775 leads to tumor inhibition and enhances efficacy of gemcitabine in human sarcomas. PLoS One. 2013; 8(3):e57523. [PubMed: 23520471]
40. Bridges KA, Hirai H, Buser CA, Brooks C, Liu H, Buchholz TA, et al. MK-1775, a novel Wee1 kinase inhibitor, radiosensitizes p53-defective human tumor cells. Clin Cancer Res. 2011 Sep 1; 17(17):5638–48. [PubMed: 21799033]
41. Hirai H, Arai T, Okada M, Nishibata T, Kobayashi M, Sakai N, et al. MK-1775, a small molecule Wee1 inhibitor, enhances anti-tumor efficacy of various DNA-damaging agents, including 5-fluorouracil. Cancer Biol Ther. 2010 Apr 1; 9(7):514–22. [PubMed: 20107315]
42. Foroutan P, Kreahling JM, Morse DL, Grove O, Lloyd MC, Reed D, et al. Diffusion MRI and novel texture analysis in osteosarcoma xenotransplants predicts response to anti-checkpoint therapy. PLoS One. 2013; 8(12):e82875. [PubMed: 24358232]
43. Harris PS, Venkataraman S, Alimova I, Birks DK, Balakrishnan I, Cristiano B, et al. Integrated genomic analysis identifies the mitotic checkpoint kinase WEE1 as a novel therapeutic target in medulloblastoma. Mol Cancer. 2014; 13:72. [PubMed: 24661910]
44. Rajeshkumar NV, de OE, Ottenhof N, Watters J, Brooks D, Demuth T, et al. MK-1775, a potent Wee1 inhibitor, synergizes with gemcitabine to achieve tumor regressions, selectively in p53-deficient pancreatic cancer xenografts. Clin Cancer Res. 2011 May 1; 17(9):2799–806. [PubMed: 21389100]
45. Carrassa L, Chila R, Lupi M, Ricci F, Celenza C, Mazzoletti M, et al. Combined inhibition of Chk1 and Wee1: in vitro synergistic effect translates to tumor growth inhibition in vivo. Cell Cycle. 2012 Jul 1; 11(13):2507–17. [PubMed: 22713237]
46. Beck H, Nahse-Kumpf V, Larsen MS, O'Hanlon KA, Patzke S, Holmberg C, et al. Cyclin-dependent kinase suppression by WEE1 kinase protects the genome through control of replication initiation and nucleotide consumption. Mol Cell Biol. 2012 Oct; 32(20):4226–36. [PubMed: 22907750]
47. Kellogg DR. Wee1-dependent mechanisms required for coordination of cell growth and cell division. J Cell Sci. 2003 Dec 15; 116(Pt 24):4883–90. [PubMed: 14625382]
48. Krajewska M, Heijink AM, Bisselink YJ, Seinstra RI, Sillje HH, de Vries EG, et al. Forced activation of Cdk1 via wee1 inhibition impairs homologous recombination. Oncogene. 2013 Jun 13; 32(24):3001–8. [PubMed: 22797065]
49. Weisberg E, Nonami A, Chen Z, Liu F, Zhang J, Sattler M, et al. Identification of Wee1 as a novel therapeutic target for mutant RAS-driven acute leukemia and other malignancies. Leukemia. 2014 May 5.
50. The Cancer Genome Atlas Research Network. Genomic and epigenomic landscapes of adult de novo acute myeloid leukemia. N Engl J Med. 2013 May 30; 368(22):2059–74. [PubMed: 23634996]
51. Vitale I, Galluzzi L, Castedo M, Kroemer G. Mitotic catastrophe: a mechanism for avoiding genomic instability. Nat Rev Mol Cell Biol. 2011 Jun; 12(6):385–92. [PubMed: 21527953]
52. Beck H, Nahse V, Larsen MS, Groth P, Clancy T, Lees M, et al. Regulators of cyclin-dependent kinases are crucial for maintaining genome integrity in S phase. J Cell Biol. 2010 Mar 8; 188(5): 629–38. [PubMed: 20194642]
53. Varmeh S, Manfredi JJ. Inappropriate activation of cyclin-dependent kinases by the phosphatase Cdc25b results in premature mitotic entry and triggers a p53-dependent checkpoint. J Biol Chem. 2009 Apr 3; 284(14):9475–88. [PubMed: 19136558]
54. Hans F, Dimitrov S. Histone H3 phosphorylation and cell division. Oncogene. 2001 May 28; 20(24):3021–7. [PubMed: 11420717]
55. Kreahling JM, Gemmer JY, Reed D, Letson D, Bui M, Altiok S. MK1775, a selective Wee1 inhibitor, shows single-agent antitumor activity against sarcoma cells. Mol Cancer Ther. 2012 Jan; 11(1):174–82. [PubMed: 22084170]

56. Guertin AD, Li J, Liu Y, Hurd MS, Schuller AG, Long B, et al. Preclinical evaluation of the WEE1 inhibitor MK-1775 as single-agent anticancer therapy. Mol Cancer Ther. 2013 Aug; 12(8):1442–52. [PubMed: 23699655]

57. Thompson R, Eastman A. The cancer therapeutic potential of Chk1 inhibitors: how mechanistic studies impact on clinical trial design. Br J Clin Pharmacol. 2013 Sep; 76(3):358–69. [PubMed: 23593991]

58. Lee J, Kumagai A, Dunphy WG. Positive regulation of Wee1 by Chk1 and 14-3-3 proteins. Mol Biol Cell. 2001 Mar; 12(3):551–63. [PubMed: 11251070]

59. Davies KD, Cable PL, Garrus JE, Sullivan FX, von CI, Huerou YL, et al. Chk1 inhibition and Wee1 inhibition combine synergistically to impede cellular proliferation. Cancer Biol Ther. 2011 Nov 1; 12(9):788–96. [PubMed: 21892012]

60. Chaudhuri L, Vincelette ND, Koh BD, Naylor RM, Flatten KS, Peterson KL, et al. CHK1 and WEE1 inhibition combine synergistically to enhance therapeutic efficacy in acute myeloid leukemia ex vivo. Haematologica. 2014 Apr; 99(4):688–96. [PubMed: 24179152]

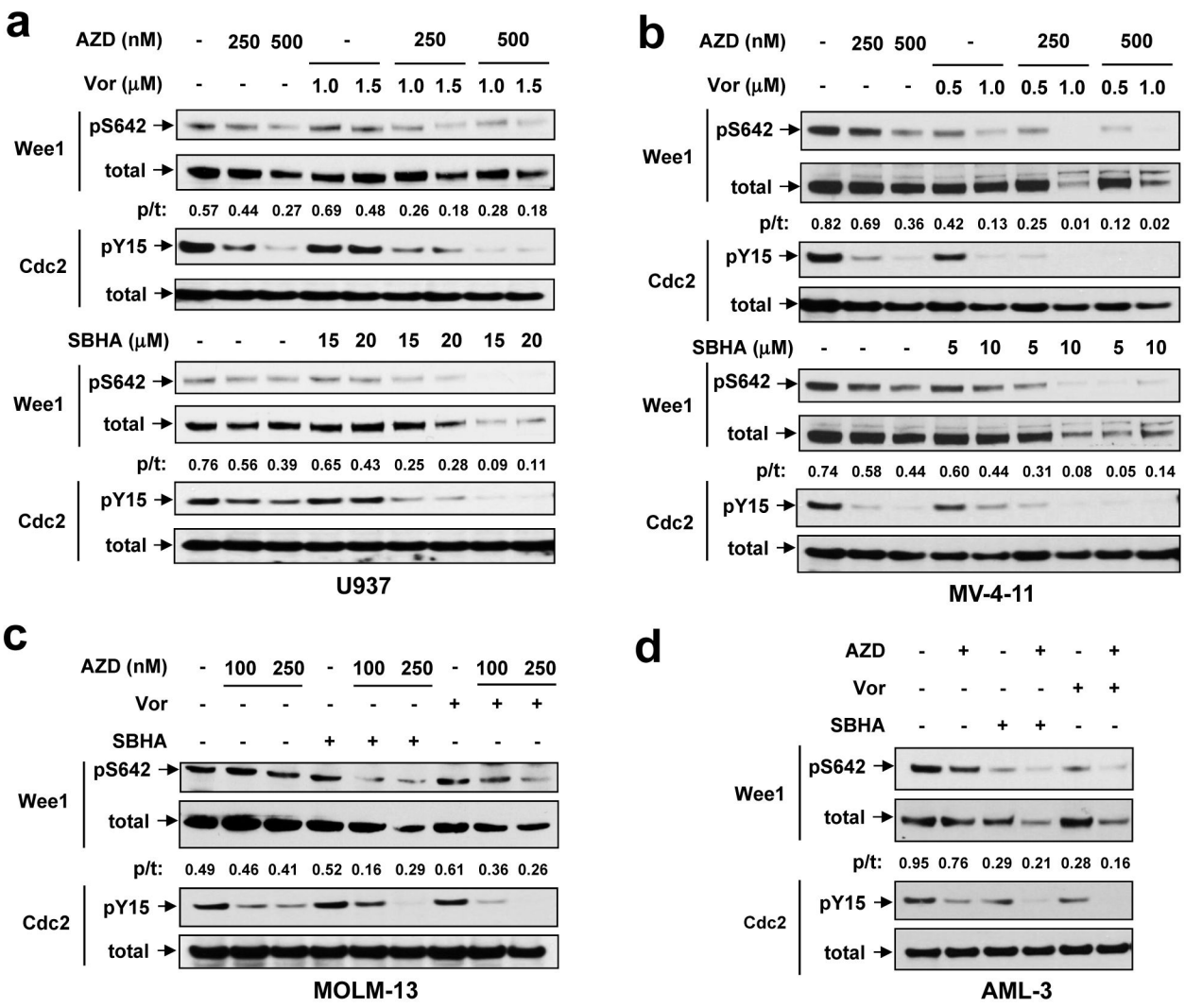

Figure 1. AZD1775 inhibits Wee1, an event enhanced by HDACIs

Human leukemia U937 (**a**), MV4-11 (**b**), MOLM-13 (**c**), and OCI-AML-3 (**d**) cells were exposed to indicated concentrations of AZD1775 +/− Vorinostat (Vor) or SBHA for 24 h, after which total and phosphorylated Wee1 (S642) and cdc2/Cdk1 (Y15) were monitored by Western blot analysis. For both MOLM-13 and OCI-AML-3, Vorinostat = 1.5 μM and SBHA = 20 μM. Blots for pWee1 (S642) and total Wee1 were quantified using ImageJ software (available online). Values indicate ratio of phosphorylated vs total Wee1.

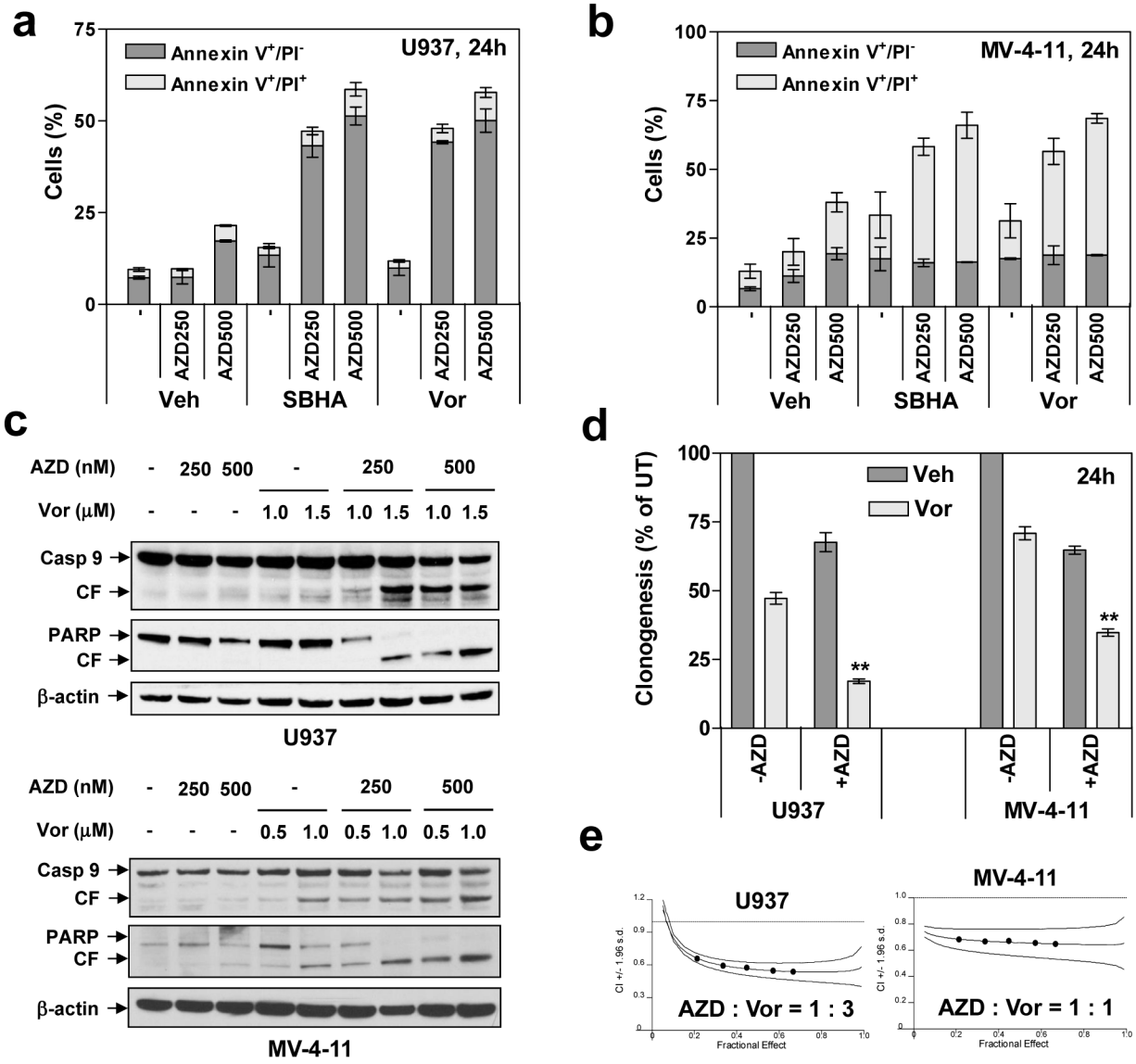

Figure 2. AZD1775 interacts synergistically with HDACIs to induce apoptosis in p53-deficient leukemia cells

(**a–b**) U937 (p53-null) and MV4-11 ($p53^{mut}$, FLT-ITD) cells were exposed to AZD1775 (nM) +/− 1.5μM Vorinostat or 15 μM SBHA for 24 h, after which the percentage of Annexin V^+/PI^- (early apoptosis) and Annexin V^+/PI^+ (late apoptosis) was determined by flow cytometry. (**c**) Alternatively, Western blot analysis was performed to detect cleavage of caspase-9 and PARP. CF = cleaved fragment. (**d**) After 24 h-exposure to AZD1775 (U937, 500 nM; MV4-11, 250 nM) +/− Vorinostat (U937, 1.5 μM; MV4-11, 0.5 μM), a soft-agar assay was performed to assess colony formation capacity (** $P < 0.01$). (**e**) Cells were exposed (24 h) to varying concentrations of AZD1775 and Vorinostat alone and in combination at a fixed ratio. At the end of this period, the percentage of Annexin V^+ cells was determined for each condition, and Median Dose-Effect analysis was then employed to characterize the nature of the interaction between these agents. Combination Index (C.I.)

values less than 1.0 denote a synergistic interaction. The results are representative for three separate experiments.

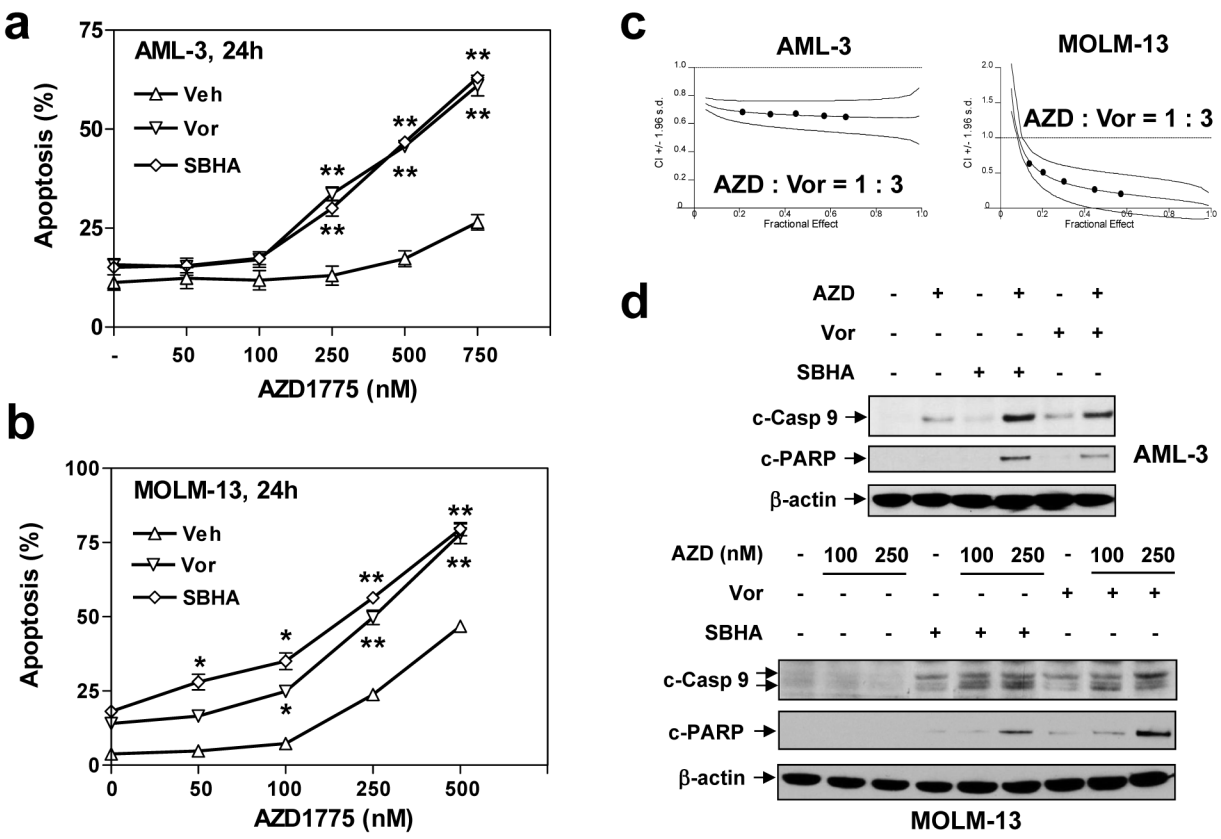

Figure 3. AZD1775 significantly potentiates HDACI lethality in leukemia cells expressing wild type p53

(**a–b**) OCI-AML-3 ($p53^{wt}$) and MOLM-13 ($p53^{wt}$, FLT3-ITD) cells were exposed to the indicated concentrations of AZD1775 +/− 1.5 μM Vorinostat or 20 μM SBHA for 24 h, after which apoptosis was monitored by Annexin V/PI staining and flow cytometry (*P < 0.05, **P < 0.01). (**c**) Median Dose-Effect analysis was performed to determine C.I. values (< 1.0 denote synergism) in OCI-AML-3 and MOLM-13 cells. The results are representative for three separate experiments. (**d**) After OCI-AML-3 and MOLM-13 cells were treated with 250 nM AZD1775 +/− 1.5 μM Vorinostat or 20 μM SBHA for 24 h, Western blot analysis was performed to monitor cleavage of caspase 9 and PARP.

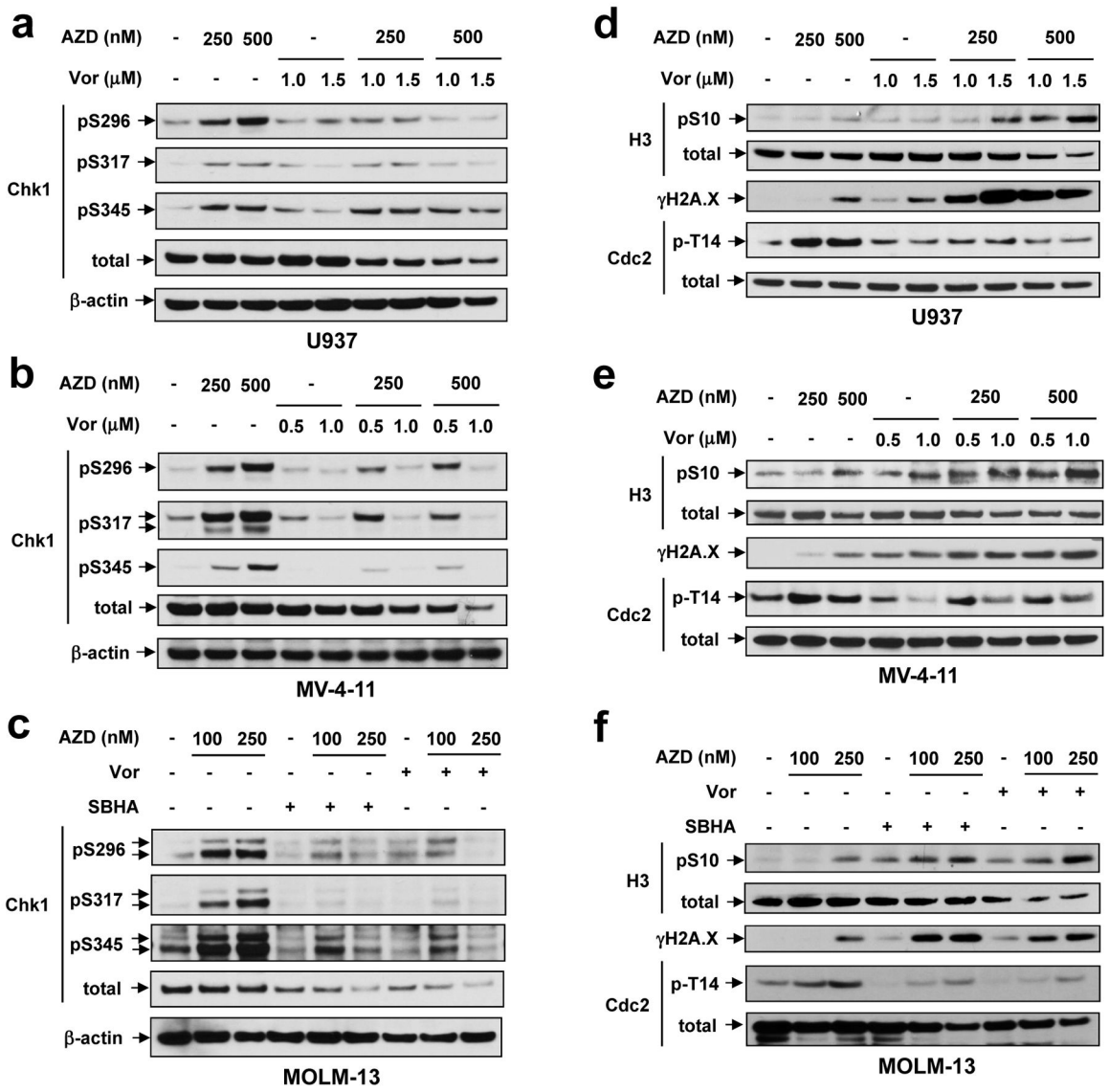

Figure 4. Exposure to AZD1775 results in Chk1 activation and cdc2/Cdk1 T14 phosphorylation, events blocked by HDACIs

(**a–c**) U937 (**a**), MV-4-11 (b), and MOLM-13 (**c**) cells were treated (24 h) with the indicated concentrations of AZD1775 +/− Vorinostat or SBHA, after which Western blot analysis was performed to examine phosphorylation (S296, S317, S345) and protein levels of Chk1. (**d–f**) Alternatively, the mitotic entry marker histone H3 S10 phosphorylation, T14 phosphorylation of cdc2/Cdk1, and total protein levels were monitored in parallel.

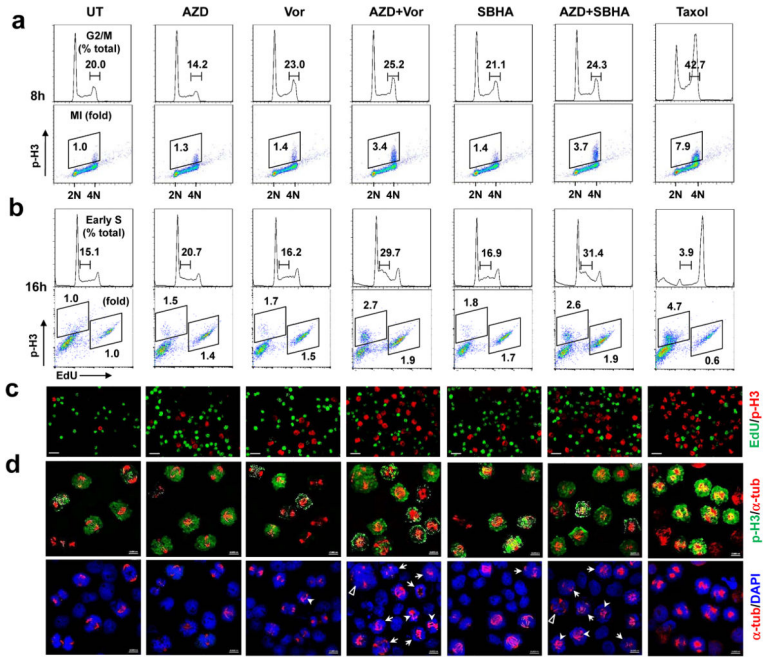

Figure 5. Co-treatment with AZD1775 and HDACIs triggers premature mitotic entry and increases newly replicated DNA in early S phase

(**a**) U937 cells were treated with 250 nM AZD1775 +/− 1.5 μM Vorinostat or 15 μM SBHA for 8 h, after which cells were stained with AlexaFluor 488-conjugated anti-phospho-histone H3 (S10) and PI to determine cell cycle distribution (top, values indicate percentage of cells in G2/M) and the percentage of p-H3-positive cells (bottom, values indicate fold-increases in p-H3-positive cells vs untreated controls) by flow cytometry. (**b**) After 16 h-treatment, cells were pulse labeled with EdU for 30 min, followed by staining for cell cycle distribution (top, values indicate percentage of cells in early S) or double staining for p-H3 and EdU (bottom, values indicate fold-increases in p-H3-positive cells and EdU-positive cells vs untreated controls, respectively). (**c–d**) Alternatively, cytospin slides were prepared, followed by triple staining for p-H3 (red), EdU (green), and α-tubulin (red) together with DAPI (blue) nuclear counterstaining. Representative images of p-H3/EdU (top) and α-tubulin/DAPI (bottom) in the same field were shown for each condition. Arrow head, anaphase bridge; arrow, monopolar or multiple spindle; triangle, centrosome clustering and mitotic slippage).

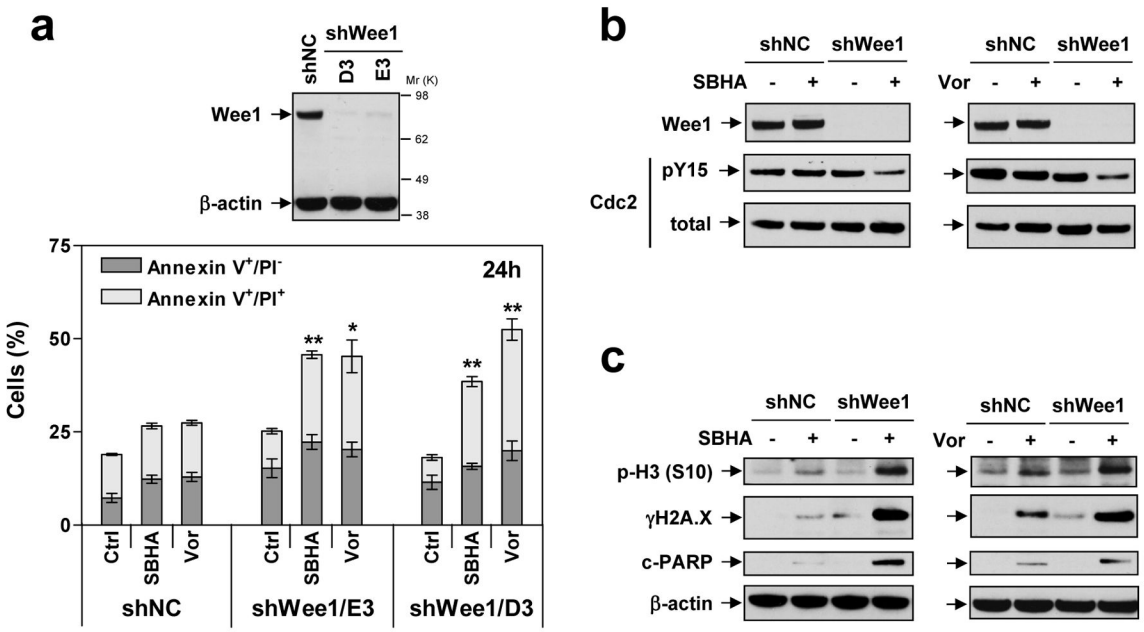

Figure 6. Knock-down of Wee1 sensitizes leukemia cells to HDACI lethality in association with premature mitotic entry and increased DNA damage

(**a**) U937 cells were stably transfected with constructs encoding shRNA targeting human Wee1 (shWee1) or scrambled sequence as negative control (shNC). Two clones (designated D3 and E3) of shWee1 cells displayed marked down-regulation of Wee1, compared to shNC cells (inset). Cells were then exposed to 1.5 μM Vorinostat or 20 μM for 24 h, after which the percentage of Annexin V^+/PI^- and Annexin V^+/PI^+ were determined by flow cytometry (*$P < 0.05$ and *$P < 0.01$ vs shNC cells). (**b–c**) Alternatively, Western blot analysis was performed to monitor levels of Wee1 and total and Y15 phosphorylated cdc2/Cdk1 (B), or phosphorylated histone H3 (S10), γH2A.X, and PARP cleavage (**c**).

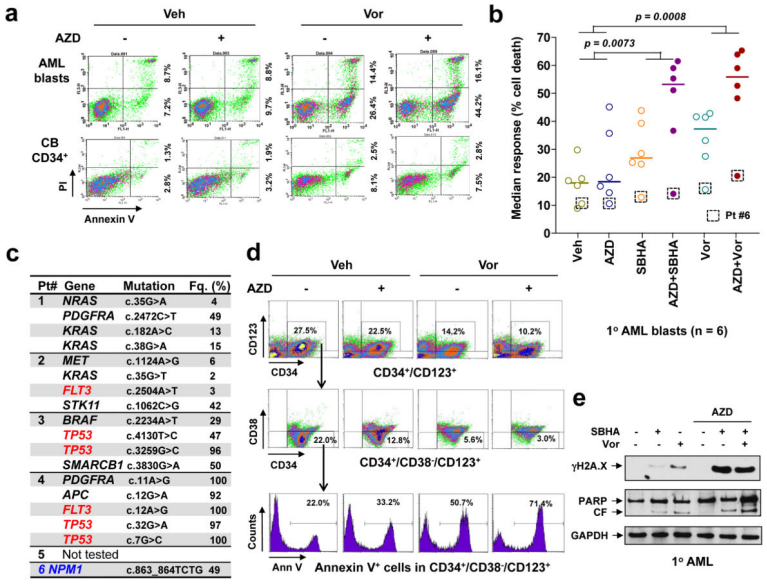

Figure 7. The AZD1775/Vorinostat regimen is active against primary AML cells, including the primitive CD34$^+$/CD38$^-$/CD123$^+$ population, but displays minimal toxicity towards normal CD34$^+$ cells

(**a**) Primary blasts from a patient with AML (top) and normal CB CD34$^+$ cells (bottom) were exposed to 250 nM AZD1775 +/− 1.5 μM Vorinostat for 24 h, after which cells were stained with Annexin-V/PI and analyzed by flow-cytometry. Values indicate the percentage of Annexin V$^+$/PI$^-$ and Annexin V$^+$/PI$^+$ cells in a total of 10,000 cells analyzed for each condition. (**b**) Parallel experiments were carried out with six AML primary samples. Median response was analyzed based on the percentage of cell death measured by $DiOC_6$/7AAD double staining and flow cytometry. Squares highlight the weakly-responding sample expressing only the NPM1 mutation (patient #6; see panel c). P values were determined by One-way ANOVA with Tukey-Kramer Multiple Comparisons Test. (**c**) In five of these six AML patient samples, NGS was conducted to define genetic abnormalities using the Cancer Hotspot Panel. Fq. = frequency of the mutations. (**d**) Bone marrow mononuclear cells from a primary AML sample were stained with CD132-APC, CD38-PerCP, CD34-PE, and Annexin-V-FITC, after which the percentage of apoptosis was determined in the primitive CD34$^+$/CD38$^-$/CD123$^+$ population. (**e**) Western blot analysis was performed to monitor γH2A.X levels and PARP degradation in one representative primary responding sample.

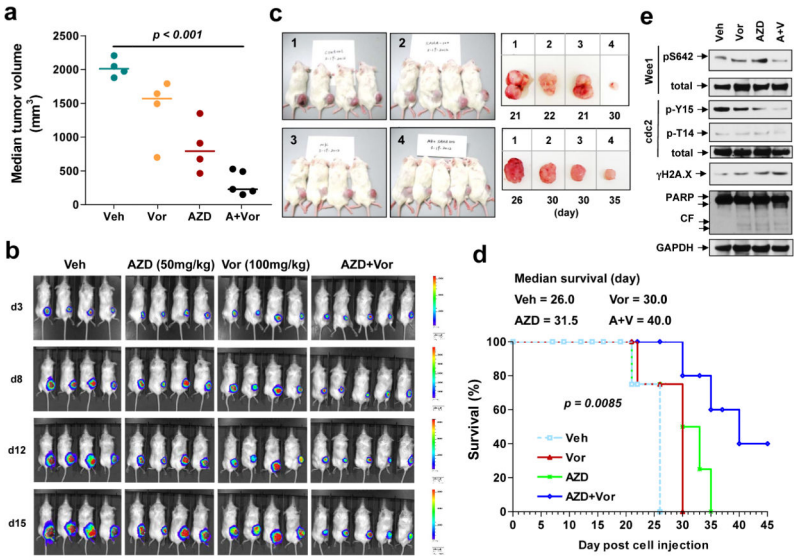

Figure 8. The combination of AZD1775 and Vorinostat suppresses tumor growth in a murine xenograft model and prolongs animal survival

NOD/SCID-gamma (NSG) mice were subcutaneously inoculated in the right rear flank with 5×10^6 U937 cells stably expressing luciferase. Treatment was initiated after luciferase activity was detected (5 days after injection of tumor cells). AZD1775 was freshly reconstituted with 0.5% methylcellulose and administrated at a dose of 50 mg/kg by oral gavage (p.o.) bid three days a week. Vorinostat in DMSO was diluted in PEG/H2O (1:1) and administrated at a dose of 100 mg/kg via intraperitoneal (i.p.) injection daily five days a week. Control animals were administered equal volumes of vehicle. (**a**) Tumor size was measured visually every other day. Representative median tumor volume for day 21 was shown. (**b**) Tumor growth was monitored every other day after i.p. injection with 150 mg/kg luciferin using the IVIS 200 imaging system. d = day. (**c**) Representative images of mice (day 21) and tumors removed from mice on the indicated day post-tumor cell injection. 1 = vehicle, 2 = 100 mg/kg Vorinostat, 3 = 50 mg/kg AZD1775, 4 = AZD1775 + Vorinostat. (**d**) Kaplan-Meier analysis performed to analyze survival of animals. Inset, median survival. (e) Tumor tissues were homogenized and subjected to Western blot analysis.